Pressure and Drag-Driven Flow Between Two Infinite Parallel Flat Plates

Presented to : Professor Phillip Servio

Prepared by

Ngan Jennifer Tram Su [260923530]

CHEE 390 – Computational Methods in Chemical Engineering

Department of Chemical Engineering

McGill University

2021.11.23

Table of Contents

Nomenclature

$v_x(y)(\frac{m}{s})$	Velocity profile as a function of y
$v_{x_0}\ (\frac{m}{s})$	Velocity at $y = 0$
$v_{x_B}\ (\frac{m}{s})$	Velocity at $y = B$
$\mu\ (Pa \cdot s)$	Newtonian Viscosity
$\rho\ (\frac{kg}{m^3})$	Density of an incompressible fluid
$\frac{\Delta P}{\Delta x}\ (\frac{Pa}{m})$	Constant pressure gradient
$< v_x >$	Average velocity

1 Objective

The equation of motion is a partial differential equation that can be used to describe fluid flow; it combines the contributions of time, convection, shear stresses, and surface and body forces. In this investigation, the flow of an incompressible Newtonian fluid between two infinite parallel plates separated by a distance B was examined (Figure 1). As well, the no-slip condition was applied, providing boundary conditions at the surface of each plate ($v_{x_0}\ and\ v_{x_B}$).

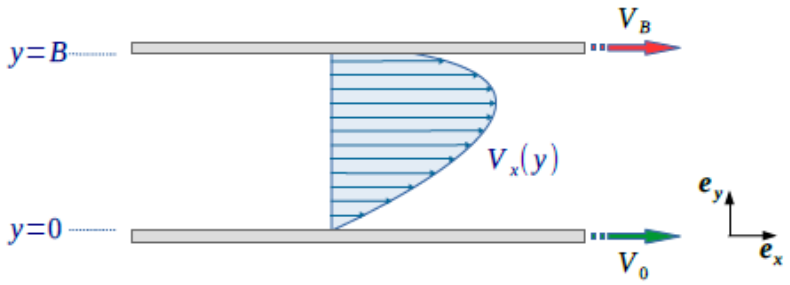

Figure 1 Pressure and Drag-Driven Flow between Two Infinite, Parallel Flat Plates

Each plate exerts a shear stress on the fluid, while the constant pressure gradient provides an additional driving force to the flow. As a result, the fluid undergoes laminar flow, where the velocity along each point in the vertical axis will vary. The objective of this report was to derive the velocity profile, the average velocity, and the Reynold's number. By changing the flow conditions, their effects on these derived parameters were explored.

2 Flowchart

Figure 2 and Figure 3 depict the flow of the main program that solves for the velocity profile, average velocity, and the Reynold's number of a Newtonian fluid under pressure-driven flow.

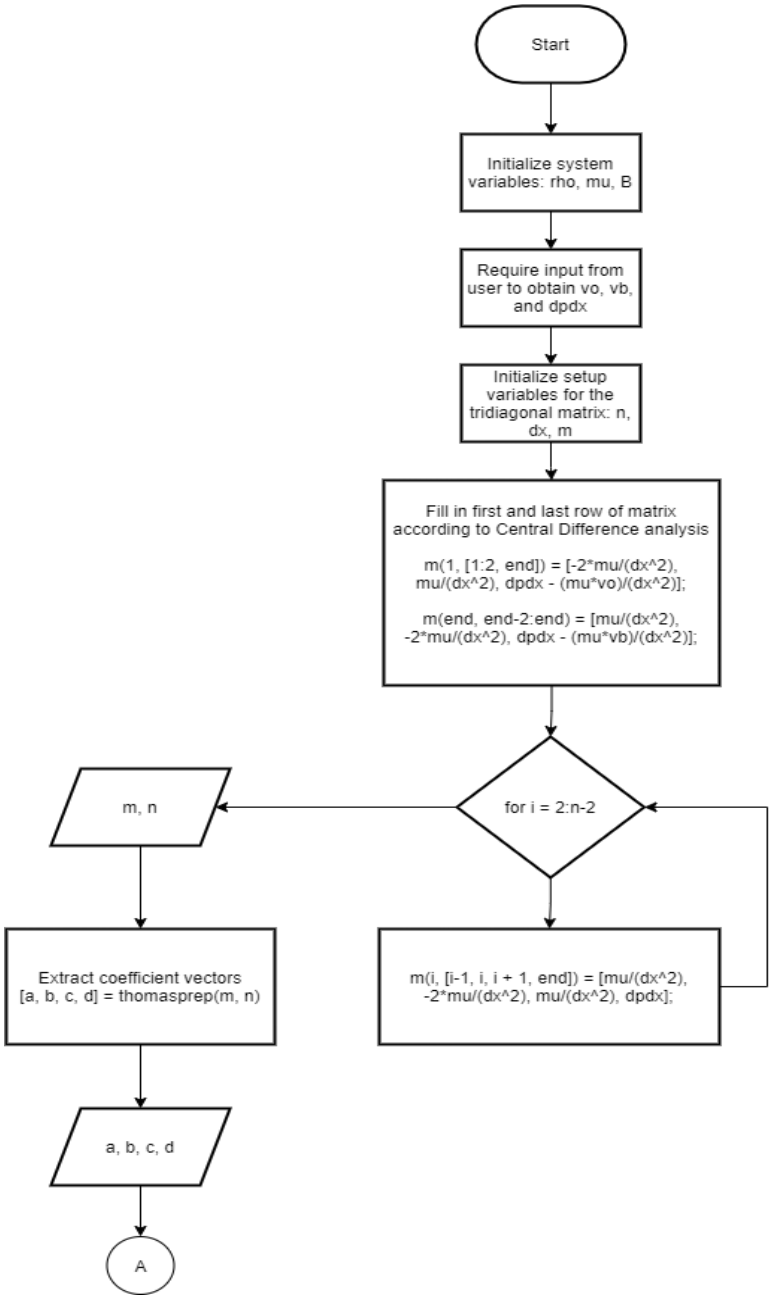

Figure 2 Main Program Flowchart (1/2)

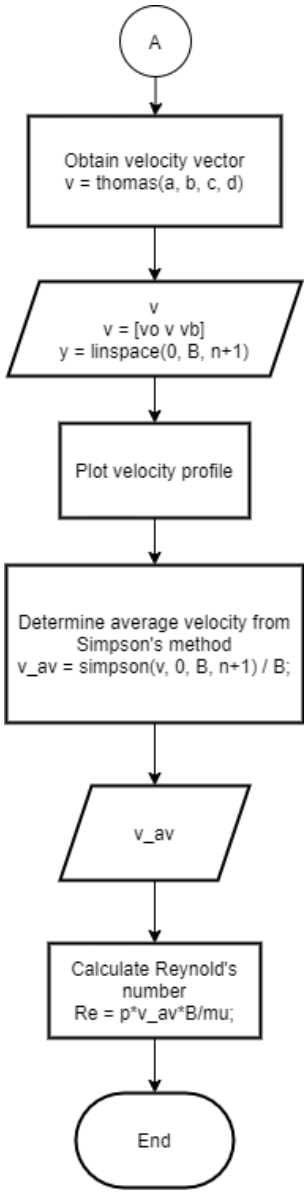

Figure 3 Main Program Flowchart (2/2)

3 Results

3.1 Velocity Profile

Pressure-driven flow of an incompressible, Newtonian fluid can be described through the Navier-Stokes equation of motion (1).

$$\rho \frac{Dv}{Dt} = \rho \frac{\delta}{\delta t} v + \rho v \cdot \nabla v = -\nabla P + \mu \nabla^2 v \tag{1}$$

The flow was assumed to be steady, dominated by viscous forces (i.e. negligible convection), one-directional along the x-axis, and fully developed. With these additional assumptions imposed, the equation of motion in the x-direction reduces to equation (2).

$$0 = -\left(\frac{\Delta P}{\Delta x}\right) + \mu \frac{d^2 v_x}{dy^2} \tag{2}$$

Finally, the no-slip condition of fluid motion presents two Dirichlet boundary conditions: v_0 and v_B, which are the fluid velocities at the lower and upper plate, respectively.

Although this system can be solved analytically, the finite difference computational method was implemented. Through the central difference analysis, the second derivative of velocity can be written as follows:

$$\frac{d^2 v_x}{dy^2} = \frac{d}{dy}\left(\frac{dv_x}{dy}\right)$$

$$\frac{d^2 v_x}{dy^2} = \frac{\frac{dv_x}{dy}\Big|_{i+\frac{1}{2}} - \frac{dv_x}{dy}\Big|_{i-\frac{1}{2}}}{\Delta y}$$

$$\frac{d^2 v_x}{dy^2} = \frac{\frac{v_{x_{i+1}} - v_{x_i}}{\Delta y} - \frac{v_{x_i} - v_{x_{i-1}}}{\Delta y}}{\Delta y}$$

$$\frac{d^2 v_x}{dy^2} = \frac{v_{x_{i+1}} - 2v_{x_i} + v_{x_{i-1}}}{\Delta y^2}$$

Where Δy is the step size between points $i \; and \; i+1$.

This expression can then be substituted into equation (2) to obtain a relation (3) between the velocity at point i, and the points adjacent to it:

$$0 = -\left(\frac{\Delta P}{\Delta x}\right) + \mu \left[\frac{v_{x_{i+1}} - 2v_{x_i} + v_{x_{i-1}}}{\Delta y^2}\right] \tag{3}$$

Between the lower and upper plate are n divisions of equal length ($n-1$ points). For this investigation, 50 divisions were used to obtain 49 points. As such, 49 linear equations were constructed through the finite difference method.

At the point $i = 1$, relation (3) yields the first linear equation:

$$0 = -\left(\frac{\Delta P}{\Delta x}\right) + \mu \left[\frac{v_{x_2} - 2v_{x_1} + v_{x_0}}{\Delta y^2}\right]$$

Where v_{x_0} is the first known boundary condition at the lower plate.

To facilitate analysis, terms were rearranged as to isolate the unknown variables from the known constants:

$$-\frac{2\mu}{\Delta y^2} v_{x_1} + \frac{\mu}{\Delta x^2} v_{x_2} = \frac{\Delta P}{\Delta x} - \frac{\mu}{\Delta x^2} v_0$$

Similarly, at the point $i = n-1$, relation (3) yields the final linear equation:

$$0 = -\left(\frac{\Delta P}{\Delta x}\right) + \mu \left[\frac{v_{x_n} - 2v_{x_{n-1}} + v_{x_{n-2}}}{\Delta y^2}\right]$$

Where $v_{x_n} = v_{x_B}$ is the second known boundary condition at the upper plate.

$$\frac{\mu}{\Delta x^2} v_{x_{n-2}} - \frac{2\mu}{\Delta x^2} v_{x_{n-1}} = \frac{\Delta P}{\Delta x} - \frac{\mu}{\Delta x^2} v_{x_B}$$

Finally, for the points in-between the boundaries ($i = 2 \dots n-2$), relation (3) can be manipulated into a more usable form:

$$0 = -\left(\frac{\Delta P}{\Delta x}\right) + \mu \left[\frac{v_{x_{i+1}} - 2v_{x_i} + v_{x_{i-1}}}{\Delta y^2}\right]$$

$$\frac{\mu}{\Delta x^2} v_{x_{i-1}} - \frac{2\mu}{\Delta x^2} v_{x_i} + \frac{\mu}{\Delta x^2} v_{x_{i+1}} = \frac{\Delta P}{\Delta x}$$

From these linear equations, a tridiagonal matrix was constructed and solved using the Thomas algorithm.

To explore the effects of varying Dirichlet boundary conditions and constant pressure gradients, five scenarios were proposed and are summarized below in Table 1.

Table 1 Scenarios with Varying Dirichlet Boundaries and Constant Pressure Gradients

Scenario	$\boldsymbol{v_{x_0}}\ \left(\frac{\boldsymbol{m}}{\boldsymbol{s}}\right)$	$\boldsymbol{v_{x_B}}\ \left(\frac{\boldsymbol{m}}{\boldsymbol{s}}\right)$	$\frac{\boldsymbol{\Delta P}}{\boldsymbol{\Delta x}}\ \left(\frac{\boldsymbol{Pa}}{\boldsymbol{m}}\right)$
1	0	0	-1
2	0	0	-5
3	4e-5	1e-4	-1
4	4e-5	1e-4	0
5	3e-5	-1e-4	-1

The velocity profiles for each of these scenarios may be accessed in section 6 Appendi.

3.2 Average Velocity

For each scenario, the average velocity was computed through the centroid method (4) and summarized in Table 2.

$$< v_x > = \frac{\int v_x dA}{\int dA} \tag{4}$$

Assuming that the plates have width w along the z-axis, the cross-sectional area may be written as $A = wB$.

$$< v_x > = \frac{\int_0^B v_x w dy}{\int_0^B w\, dy}$$

$$< v_x > = \frac{\int_0^B v_x dy}{B}$$

Where the integral in the numerator was solved through Simpson's method with $n = 51$ points (50 intervals).

3.3 Reynold's Number

Reynold's number is a dimensionless parameter that describes the ratio of inertial forces to viscous forces.

$$Re = \frac{\rho v D}{\mu} \tag{5}$$

Where ρ is the fluid density, v is the velocity, D is a characteristic length associated with the volume of the fluid, and μ is the viscosity.

Large Reynold's numbers indicate a dominance in inertial forces, while the inverse indicates overwhelming viscous forces.

Through the average velocity, the Reynold's number for each scenario was calculated, which may also be found in Table 2.

Table 2 Average Velocity and Reynold's Number for Each Scenario

Scenario	$< v_x > \left(\frac{m}{s}\right)$	Re
1	8.333e-5	0.08333
2	4.167e-4	0.41667
3	1.533e-4	0.15333
4	7.000e-5	0.07000
5	4.833e-5	0.04833

4 Discussion

4.1 Scenario Comparison

Scenarios 1 and 2 have the same boundary conditions but different pressure gradients. As seen in Figure 4 and Figure 5, although these scenarios have the same velocity profile, their average velocities and Reynold's number were different, with both parameters being higher in Scenario 2. As previously mentioned, higher Reynold's numbers indicate that the flow is more dominated by inertial forces than viscous. Both scenarios have no shear stresses present (non-moving plates), and the pressure gradient is higher in scenario 2. As such, the net forces contributing to fluid flow in scenario 2 are greater than that of scenario 1, resulting in increased momentum and thus, more inertial forces.

Scenario 3 differs from scenario 1 in that neither of the plates are stationary. As a result, while the velocity profile retains the same parabolic shape, it is not a symmetric curve about the horizontal axis (Figure 6). However, as another driving force is present, the inertial forces present are greater, resulting in a higher average velocity and thus, higher Reynold's number.

Of all the scenarios, only scenario 4 has a constant pressure gradient of 0. Consequently, fluid flow is reduced to being the pure result of shear stresses exerted from the top and bottom plates. With no pressure driving the flow from behind, the velocity profile (Figure 7) reduces to a linear profile.

The plates move in opposite directions for scenario 5, and as a result, the velocity profile crosses into negative values, indicating flow in the opposite direction. Noticeably, some of the parabolic profile also remains present, and is attributed by the pressure gradient. This scenario also presents the lowest average velocity and Reynold's number; as some fluid moves in the negative direction, the net velocity is lower.

4.2 Program Considerations

4.2.1 Matrix Manipulation

The finite difference method results in a tridiagonal matrix that can be solved through either Gaussian elimination or the Thomas algorithm. Between the two methods, the Thomas algorithm takes advantage of the (forward substitution) nature of tridiagonal matrices, requiring only $O(n)$ steps as opposed to $O(n^3)$. Comparatively, Gaussian elimination is much less efficient in both computational complexity and time. The tridiagonal matrix produced in scenario 1 was inputted to both methods and timed for comparison. Taking three trials, the averages of the elapsed times were compared (Table 3).

Table 3 Elapsed Time of Code Execution for Thomas Algorithm and Gaussian Elimination

	Thomas Algorithm **Time Elapsed (s)**	**Gaussian Elimination** **Time Elapsed (s)**
Run 1	0.000900	0.005762
Run 2	0.000883	0.006219
Run 3	0.000043	0.000959
Average Time Elapsed	0.000609	0.004310

The percentage difference between the two average times can thus be determined:

$$\%\, difference = \frac{t2 - t1}{t1} \cdot 100\%$$

$$\%\ difference = \frac{0.004310 - 0.000609}{0.000609} \cdot 100\%$$

$$\%\ difference = \frac{0.004310 - 0.000609}{0.000609} \cdot 100\%$$

$$\%\ difference = 607.7176\%$$

Evidently, the Thomas algorithm takes a significantly less amount of time, with the average percentage difference being approximately 600%.

4.2.2 Choice of Numerical Method for Integration

With enough halving steps, Romberg integration may produce an area of higher accuracy than Simpson's method. requiring at least 3 halving steps ($K = 3$, to give a complexity of $O(h^6)$), to surpass an accuracy of $O(h^4)$. However, Romberg integration requires two function evaluations, $f(x + h)$ and $f(x - h)$. Through the finite difference method, expressions were determined for the points along the vertical axis, leading to the construction of a tridiagonal matrix. As these points were not united by a single function, Romberg's method for integration was not applicable. Additionally, Simpson's method iteratively fits a quadratic to the function to every subinterval within the bounds of integration. For this specific problem statement, the velocity profile of an incompressible, Newtonian fluid undergoing pressure-driven flow produces a parabolic profile. As such, Simpson's method is the ideal method. The consistency in function order further reduces the truncation error, and thus, produces an area of greater accuracy than Romberg integration, regardless of the number of halving steps.

4.2.3 Odd Number of Points

Simpson's method requires an odd number of points. For each subinterval, the integrated quadratic results in the following equation (6).

$$A = \frac{h}{3}[f(x_i) + 4f(x_{i+1}) + f(x_{i+2})] \tag{6}$$

Considering the whole interval, the overlap of points results in equation (7).

$$\int_a^b f(x)dx = \frac{h}{3}\left[f(a) + f(b) + 4\sum_{i=2,4\ldots}^{n-1} f(x_i) + 2\sum_{i=3,5\ldots}^{n-2} f(x_i)\right] \tag{7}$$

Where $h = \frac{b-a}{n-1}$.

Evidently, a quadratic can only be fit when given 3 points. This is further elucidated through equation (6) as the area is centrally determined around the point x_{i+1}. Therefore, as Simpson's method iteratively constructs a quadratic for every 3-points, the total number of points present must be odd; otherwise, an interval containing only 2 points is leftover and Simpson's method is incomplete.

5 Conclusion

The velocity profile of an incompressible, Newtonian fluid is governed by shear stresses and pressure gradients. Its motion can be described through the Navier-Stokes equation, from which the profile can be derived using the finite difference approximation method. Five scenarios were proposed, whose varying parameters allowed for the investigation of their effects on the profile, average velocity, and Reynold's number. In general, it was found that pressure contributed to the parabolic profile, while pure shear stresses produced a linear profile. An increase in the magnitude of these quantities resulted in an increase in momentum, leading to a higher average velocity and Reynold's number. Additionally, the use of the finite difference method led to the formation of a tridiagonal matrix. While both Gaussian elimination and the Thomas algorithm are valid approaches, the latter is clearly the preferred method due to its specificity to tridiagonal matrices. To achieve the average velocity, v_z was integrated over the area using Simpson's method. Due to the finite nature of the problem, where no function was extracted, Romberg's integration method was not applicable. Furthermore, Simpson's method uses a 3-point quadratic approximation, matching the exact order of the parabolic shape of the velocity profiles. Consequently, the truncation error is significantly reduced, providing an estimation of higher accuracy than that of Romberg, even when at higher order approximations.

6 Appendix

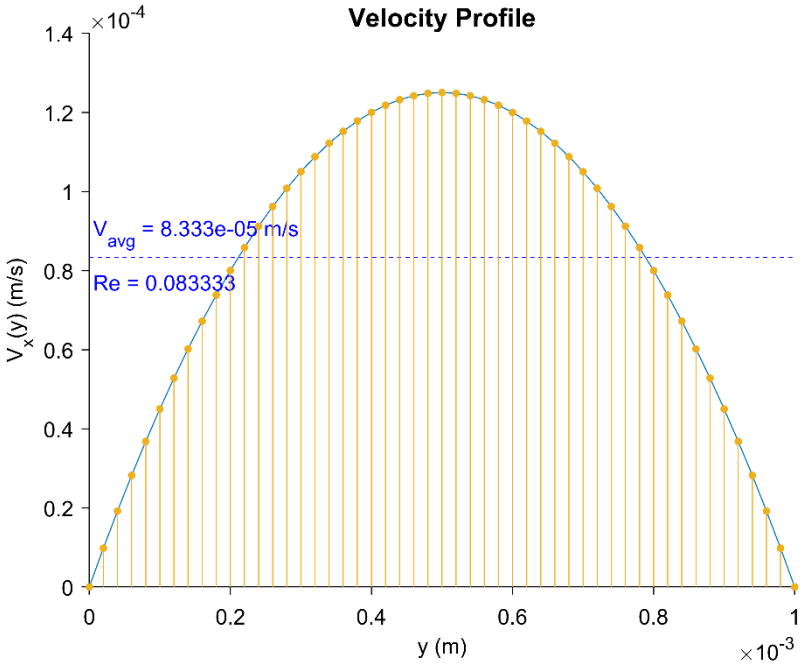

Figure 4 Velocity Profile for Scenario 1

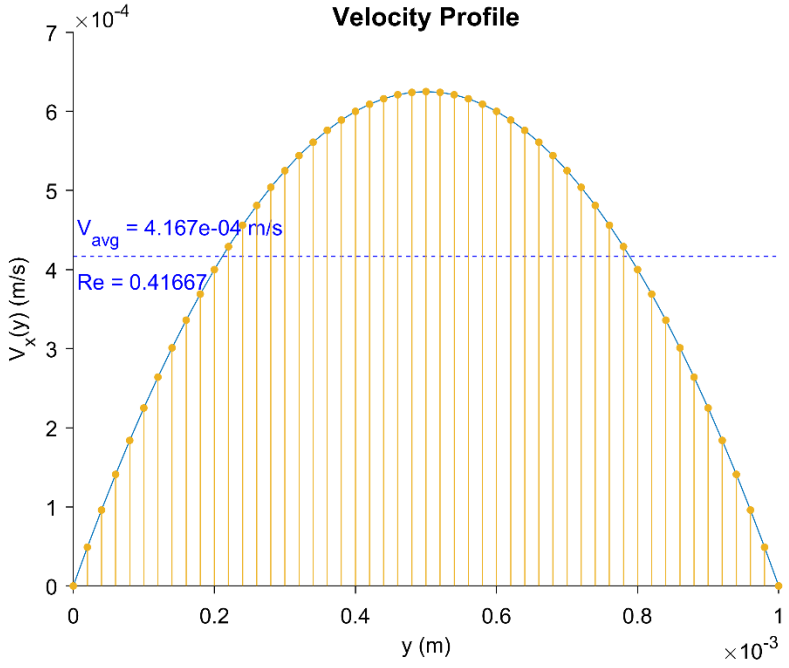

Figure 5 Velocity Profile for Scenario 2

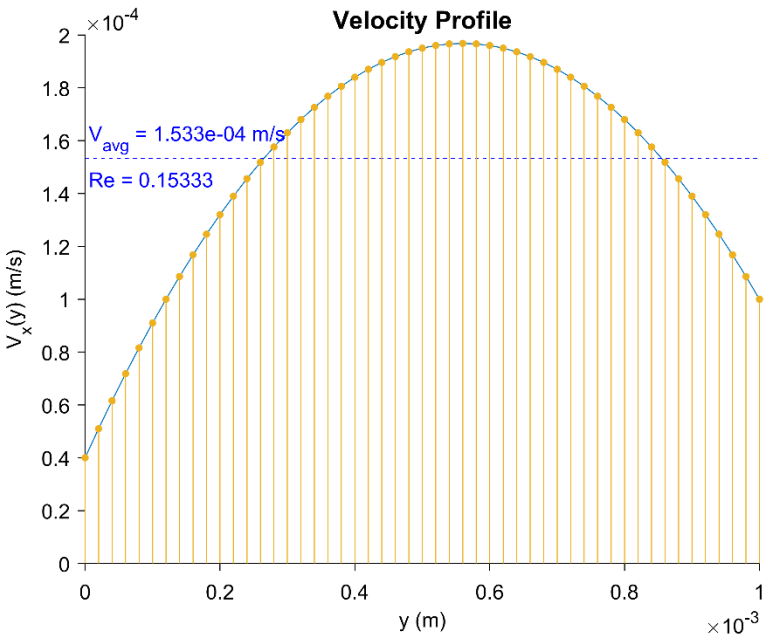

Figure 6 Velocity Profile for Scenario 3

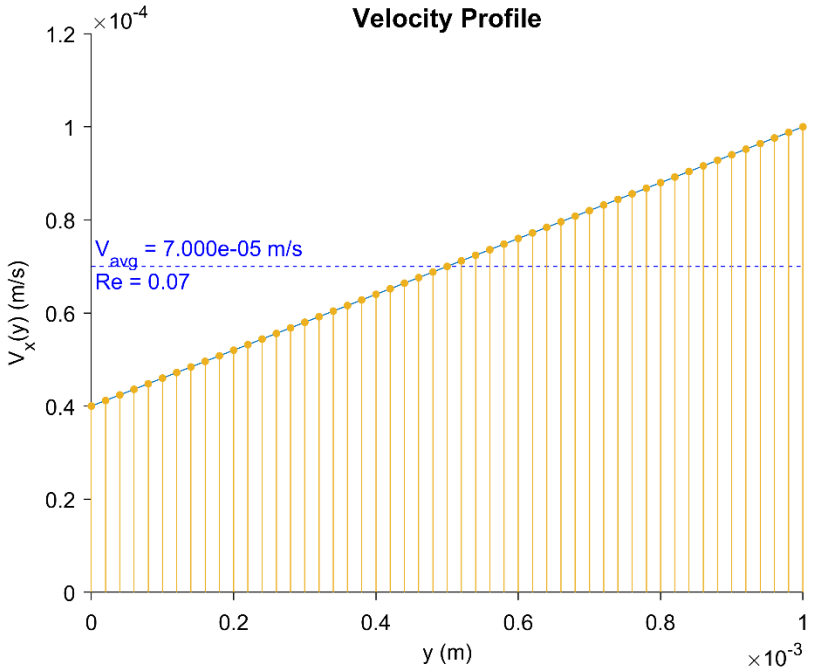

Figure 7 Velocity Profile for Scenario 4

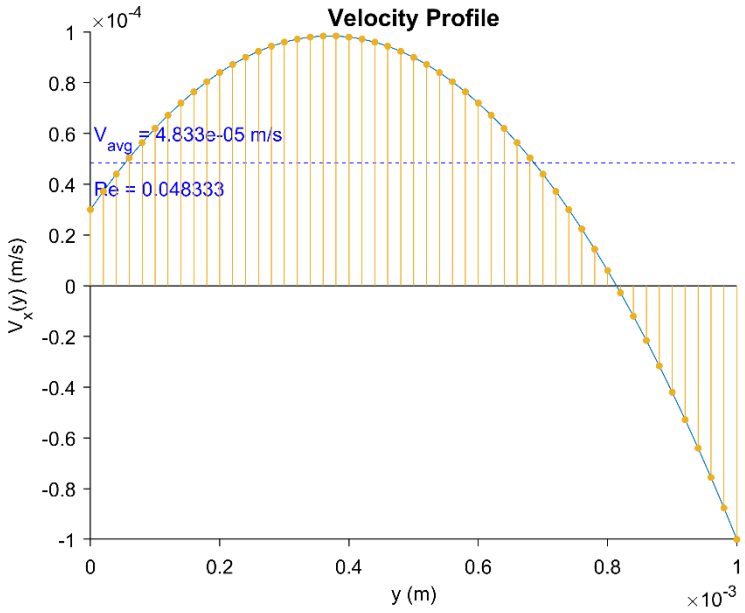

Figure 8 Velocity Profile for Scenario 5